Moroccan Journal of Chemistry
ISSN: 2351-812X
http://revues.imist.ma/?journal=morjchem&page=login
Mollaamin & al. / Mor. J. Chem. 8 N°2 (2020) 400-411

Chemotherapy Study of alkaloids through Theoretical Quantum Methods

Fatemeh Mollaamin

Department of French Language and Literature, Science and Research Branch, Islamic Azad University, Tehran, Iran

** Corresponding author:*
smollaamin@gmail.com
Received 09 June 2019,
Revised 08 April 2020,
Accepted 19 April 2020

Abstract

We know that vinblastine as one of the vinka alkaloids, has played a major role in cancer chemotherapy by inhibiting the polymerization of tubulin into microtubules. We present an in-depth investigation of the structural, infrared spectra of vinblastine. The structure of vinblastine are theoretically investigated using the density functional theory (DFT) and Hartree-Fock (HF) levels of theory with the standard 6-31G* and 6-31G** basis sets. The vibrational spectral data obtained from IR spectra are assigned modes based on the results of the theoretical calculations as intensity and frequency curves. The fundamental vibrational modes were characterized depending on their stability of vinblastine in different dielectric constants .Thermodynamic analysis of data demonstrates good correlation of vinblastine at various media by SCRF-Onsager model with linear coefficient (R^2).Thus, the goal of the work here is to evaluate and quantify the molecular basis for vinblastine structure in variant position.

Keyword: *Vinblastine, DFT, SCRF, Thermodynamic properties, Intensity, vibrational frequency*

1.Introduction

Vinca alkaloids (vinblastine, vincristine, and more recently, vinorelbine) are antimitotic, anticancer agents that induce tubulin to form spiral polymers at physiological protein concentrations. Sedimentation velocity to investigate the effects of six vinca alkaloids on tubulin spiraling. Thermodynamic analysis of LnK_1K_2 data demonstrates large and positive ΔS values, indicating that tubulin spiral formation is entropically- driven [1]. Quantitatively examined the Additivity of Dilantin and Vinblastine Inhibitory Effects on Microtubule Assembly1 [2].The interaction of vinblastine with calf brain tubulin has been studied by velocity sedimentation, gel filtration, and fluorescence [3].Then discuss the Physiochemical Aspects of Tubulin- interacting Antimitotic Drugs [4].The interactions of vinblastine with tubulin heterodimers and microtubules have been studied extensively, and in Vitro studies have shown that at low ionic strengths vinblastine induces spiral formation by a mechanism involving ligand-mediated plus ligand-facilitated isodesmic self-association [5].Tryptic hydrolysis identifies a single fluorescent β-peptide coinciding with residues 175–213 [6]. A new quinuclidine betaine (1-carboxymethyl-quinuclidinium inner salt), QNB, has been synthesized and characterized by X-ray diffraction, FTIR, NMR, and Raman spectra, and DFT calculations [7]. Combined experimental and computational vibrational spectra of 5-aminoquinoline (5-AQ) and its zinc chloride complex {Zn (5-AQ) $2Cl_2$}, together with the computational results of 5-AQ interacting with H2O through the ring nitrogen {5-AQ_H2O} have been reported. The geometry of the free 5-AQ were optimized using DFT method at B3LYP/6-31G (d, p) and 6-31++G (d, p) levels of theory [8]. The theoretically possible stable conformers of free mn-15S2O3 maleonitrile-dithiacrown ether molecule were searched by means of a conformational study which consists of molecular dynamics and energy minimization calculations performed with MM2 force field and successive geometry optimization + frequency calculations performed first at B3LYP/3-21G and then at B3LYP/6-31G(d) levels of theory [9]. Density functional theory (DFT) was used to calculate a distribution of unpaired-electron spin density for monomer radical cations to predict the coupling positions during polymerization. This method allowed to resolve the problems concerning the monomer linkage, still present after analysis of FTIR spectra of the polymer [10].The vibrational wavenumbers of the 4-chloro-2-(3,4-dichlorophenylcarbamoyl)phenyl acetate have been computed on the basis of density functional theory using B3LYP/6-31G* basis set [11]. The structural optimization and normal mode analysis were performed for P'_0 dendrimer on the basis of the density functional theory (DFT) [12].The structure of the Schiff base derived from 2-hydroxy-1-naphthaldehyde and methylamine has been studied by X-ray diffraction, B3LYP/6-31G (d,p) calculations, NMR and FTIR spectroscopy [13]. FT-IR and Raman techniques were employed for the vibrational characterization of the food additive Carmoisine (E122). The equilibrium geometry, various bonding features, and harmonic vibrational wavenumbers have been investigated with the help of density functional theory (DFT) calculations [14]. In this paper we report the IR spectra study combined with DFT calculations of the most important part of vinblastine which consists eight atoms. This work is an extension of the spectroscopic and quantum chemical studies concerning the structure and reactivity of vinblastine. The optimized structure parameters of the molecule and its IR spectra were obtained using DFT techniques.

2. Theoretical Methods

Approaches are based on Hartree-Fock (HF) and density functional theories (B3LYP method) were performed with Gaussian03 computational package [15]. The calculations employed the B3LYP exchange-correlation functional, which combines the hybrid exchange functional of Becke [16,17] with the gradient-correlation functional of Lee, Yang and Parr [18] and the split-valence polarized 6-31G(d,p) basis set [19]. In this investigation, charge distribution, geometry optimizations and thermodynamic properties were employed with different model chemistries (sto-3g, 3-21g, 6-31g, 6-31g* and 6-31g**) in various solvents (water, ethanol and methanol) at diverse temperatures (300, 305,

310, 315, 320). The most popular SCRF methods based on apparent surface charges that method is named PCM which has been extended to deal with non-electrostatic effects using scaled particle theory as formulated by Pierotti's or modified subsequently by Claverie [20,21]. Among the SCRF methods based on multipole expansions, the most popular are those developed by Rinaldi and Rivail [22-26], whose algorithm relies on the use of a rigorous multipolar expansion up to the 7th order, by Frisch, The method is currently available at both semiempirical and ab initio levels. In ordinary chemistry, a system contains more than one component, and major and minor components in the mixture are conventionally called “solvent” and “solute”, respectively. The vanishing limit of solute concentration, or infinite dilution, is of particular interest because it purely reflects the nature of solute-solvent interactions. The seminal papers of Kirkwood [27, 28] and Onsager [29] have provided inspiration for various continuum solvation models based on a multipole expansion (MPE) of the solute charge distribution. Appreciable popularity was gained in past years by the Onsager-SCRF, elaborated by Wiberg and co-workers [30, 31] for the Gaussian program. The Onsager model is the simplest version of the MPE approach. Solvation is described in terms of a dipole moment, drawn in an iterative way from QM calculations on the molecule. The appealing feature of Onsager-SCRF was that it permitted one to directly exploit almost all of the computational facilities of the Gaussian packages. For its very limited computational cost, it is still in use by people not requiring an accurate description of solvation effects but just a guess or a qualitative correction to the values obtained for the isolated molecule. Users must be aware of the limitations of the approach, of the unphysical deformation of the solute charge distribution it may induce, and of other shortcomings specific of the approach, such as the lack of solvation for solutes with zero permanent dipole. The dielectric continuum models such as the self-consistent reaction field method are efficient in taking account of long range solute–solvent electrostatic interaction and the effect of solvent polarization. An alternative which can overcome the weak points of the dielectric continuum model is the QM/MM method. Since full quantum chemical treatment of molecules is computationally too demanding, the electronic structure of the solute molecule is only treated quantum mechanically (QM) whilst the molecular mechanics (MM) is introduced to describe the solvent molecule. Data collected at 300, 305, 310, 315, and 320 K were analyzed to obtain the thermodynamic parameters ΔG, ΔH, ΔS.

We have presented a comparison of ΔG, ΔH, ΔS and E derived from these data, including vinblastine-solvent is entropically driven via water, methanol and ethanol release . The excess chemical potential of solute, or the “solvation free energy”, at infinite dilution is of particular interest, because it is the quantity which measures the stability of solute in solvent, and because all other excess thermodynamic quantities are derived from the free energy. Even though this impels a less accurate description of the solute/solvent interface, this approximation facilitates the evaluation of energy derivatives in geometry optimizations and frequency analysis. Thus, for stable vinblastine, geometry optimization + frequency calculations were performed and the frequency and intensity of the vibrational modes were calculated with the Quantum Mechanics (QM) method and the fundamental vibrational modes were characterized by their total free energy. The calculations were performed at different levels of theory to obtain the more accurate equilibrium geometrical parameters and IR spectral data for each of the determined structure. It is assumed that including additional diffuse and polarization functions into the basis set used in the calculation always leads to considerable improvements on the obtained results in theory.

3.Results and Discussion

Vinblastine have two main chemical moieties, where the right half of structure (see Fig.1) is referred to as the catharanthine moiety and the left half of structure as the vindoline moiety. Catharanthine moiety alone can achieve 70% of the effect of the parent c ompound. The vindoline moiety alone (lower half) did not induce tubulin spirals, and these authors, therefore, suggested it may be important in anchoring the drug molecule [1].

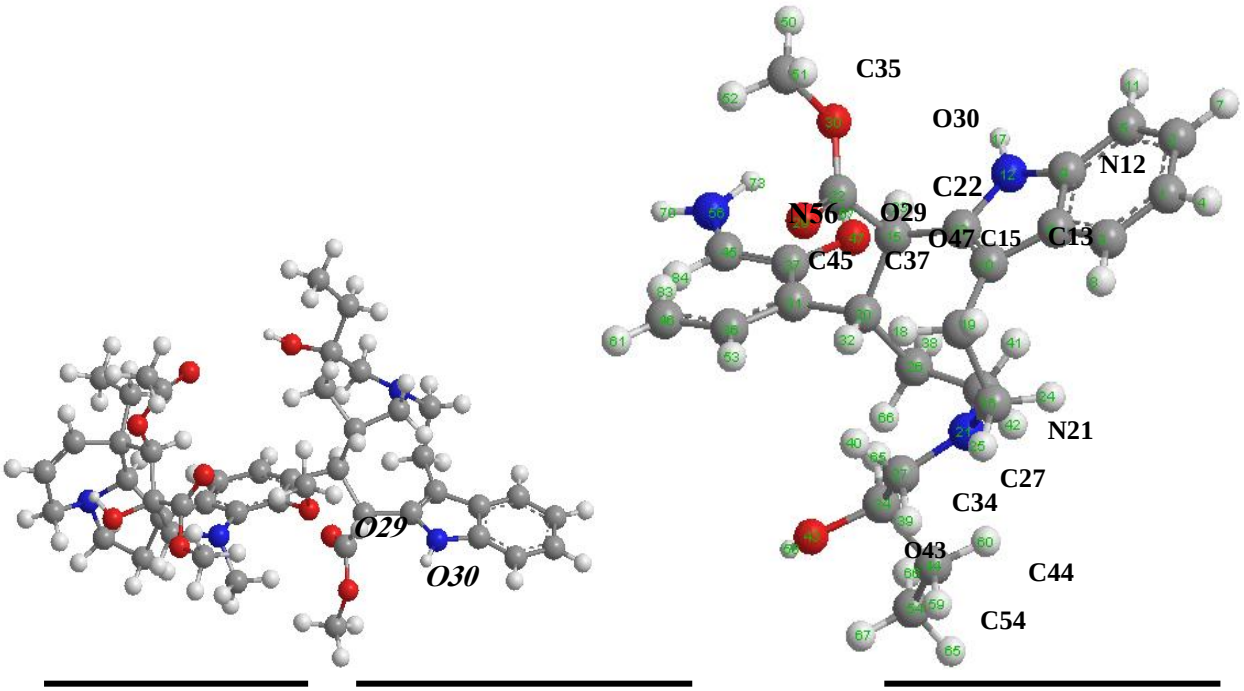

Vindoline moiety Catharanthine moiety Catharanthine moiety

Fig.1. The structures of vinblastine. Optimizations were performed by the B3LYP/6-31G method.

In the present study, we report the DFT (B3LYP)/HF calculation results for vinblastine in order to give their optimal molecular geometry and vibrational modes in several solvents and temperatures. Here, we focus on the use of modern density functional theory to fully account for the vibrational IR data for the seven atoms consisted O29 and O30 of vinblastine which have the most of Chemical shift anisotropy. The optimized configurations are shown in fig.2. The results indicate that the most stable conformation of this molecule is in water as solvent.

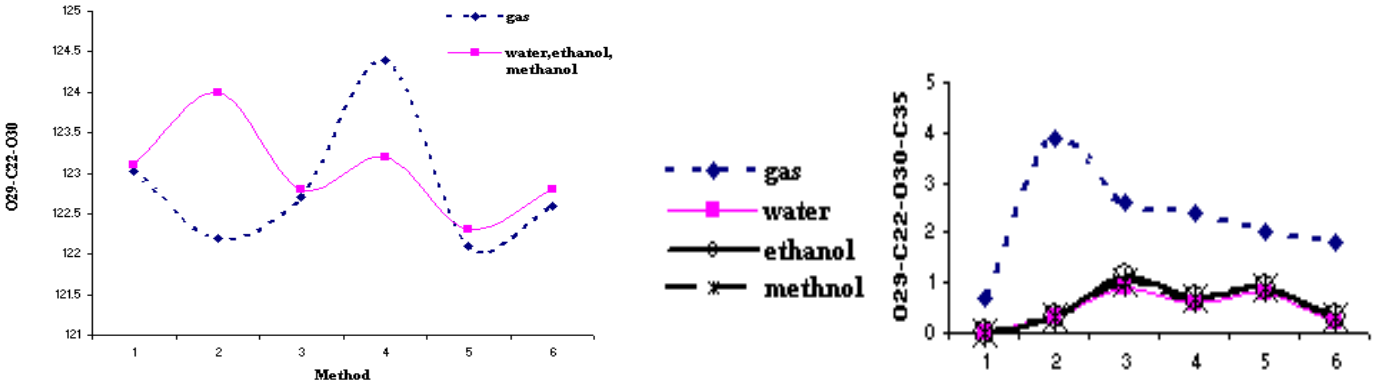

Fig. 2. Change of angles which performed by different method (**1**=HF/sto-3g, **2**=B3LYP/sto-3g, **3**=HF/3-21g, **4**=B3LYP/3-21g, **5**=HF/ 6-31g, **6**=B3LYP/6-31g).

In table 1 the calculated bond angle and dihedral angle correspond well to the different solvent phases, but as is shown in fig. 2 the behavior change of angle is completely different from gas. Using sto-3g/B3LYP method it is seen that the angle decreases in gas phase but we see different process in solvent phase and the angle increases.

Table 1. Optimized coordination of Bond Distances (Å), Bond Angles (°) and Torsion Angles (°) and stability energy of calculated Vinblastine.

HF												
Dielectric Constant	**1**			**78.39**			**32.63**			**24.55**		
Basis set	**Sto-3g**	**3-21g**	**6-31g**	**Sto-3g**	**3-21g**	**6-31g**	**Sto-3g**	**3-21g**	**6-31g**	**Sto-3g**	**3-21g**	**6-31g**
Energy	**-1652935.93**	**-1664409.72**	**-1672958.27**	**-1652940.49**	**-1664415.52**	**-1672969.74**	**-1652940.47**	**-1664411.4**	**-1672969.7**	**-1652940.46**	**-16644115.43**	**-1672969.68**
N12-C13	**1.4**	**1.4**	**1.4**	**1.4**	**1.4**	**1.4**	**1.4**	**1.4**	**1.4**	**1.5**	**1.4**	**1.4**
N12-C13-C15	**116.1**	**118.6**	**117.1**	**116.2**	**118.6**	**117.0**	**116.2**	**118.6**	**117.0**	**116.2**	**118.6**	**117.0**
N12-C13-C15-C22	**-86.4**	**-107.3**	**-99.3**	**-86.6**	**-106.9**	**-98.8**	**-86.6**	**-106.8**	**-98.8**	**-86.6**	**-106.9**	**-98.9**
O29-C22	**1.2**	**1.2**	**1.2**	**1.2**	**1.2**	**1.2**	**1.2**	**1.2**	**1.2**	**1.2**	**1.2**	**1.2**
O29-C22-O30	**123.02**	**122.7**	**122.1**	**123.1**	**122.8**	**122.3**	**123.1**	**122.8**	**122.3**	**123.1**	**122.8**	**122.3**
O29-C22-O30-C35	**0.671**	**2.6**	**2.0**	**-0.008**	**0.9**	**0.8**	**0.012**	**1.1**	**0.9**	**0.023**	**1.0**	**0.9**
N21-C27	**1.5**	**1.4**	**1.5**	**1.5**	**1.5**	**1.5**	**1.5**	**1.5**	**1.5**	**1.5**	**1.5**	**1.5**
N21-C27-C34	**112.7**	**110.9**	**112.2**	**112.6**	**110.8**	**112.0**	**112.7**	**110.8**	**112.0**	**112.6**	**110.8**	**112.0**
N21-C27-C34-O43	**-171.3**	**-174.1**	**-167.8**	**-171.0**	**-175.1**	**-169.4**	**-171.0**	**-175.2**	**-169.3**	**-171.0**	**-175.0**	**-169.3**
O43-C34	**1.4**	**1.4**	**1.4**	**1.4**	**1.5**	**1.4**	**1.4**	**1.5**	**1.4**	**1.4**	**1.5**	**1.4**
O43-C34-C44	**110.8**	**109.02**	**109.0**	**110.8**	**108.7**	**108.7**	**110.8**	**108.7**	**108.7**	**110.8**	**108.7**	**108.7**
O43-C34-C44-C54	**58.2**	**54.7**	**58.0**	**57.9**	**54.0**	**57.4**	**57.9**	**54.0**	**57.5**	**57.9**	**54.1**	**57.5**
O47-C37	**1.4**	**1.4**	**1.4**	**1.4**	**1.4**	**1.4**	**1.4**	**1.4**	**1.4**	**1.4**	**1.4**	**1.4**
O47-C37-C45	**121.7**	**120.3**	**120.5**	**121.8**	**120.6**	**120.7**	**121.8**	**120.6**	**120.7**	**121.8**	**120.6**	**120.7**
O47-C37-C45-N56	**3.4**	**-3.09**	**-2.9**	**3.2**	**-2.6**	**-3.3**	**3.2**	**-2.0**	**-3.3**	**3.2**	**-2.6**	**-3.3**
B3LYP												
Dielectric Constant	**1**			**78.39**			**32.63**			**24.55**		
Basis set	**Sto-3g**	**3-21g**	**6-31g**	**Sto-3g**	**3-21g**	**6-31g**	**Sto-3g**	**3-21g**	**6-31g**	**Sto-3g**	**3-21g**	**6-31g**
E (kcal/mol)	**-1662859.91**	**-1674876.56**	**-1683588.26**	**-1662867.04**	**-1674876.56**	**-1683592.56**	**-1662859.91**	**-1674876.56**	**-1683592.56**	**-1662859.91**	**-1674876.56**	**-1683592.56**
N12-C13	**1.4**	**1.4**	**1.4**	**1.4**	**1.4**	**1.4**	**1.4**	**1.4**	**1.4**	**1.4**	**1.4**	**1.4**
N12-C13-C15	**112.0**	**119.3**	**117.4**	**118.1**	**118.8**	**117.4**	**118.1**	**118.8**	**117.4**	**118.1**	**118.8**	**117.5**
N12-C13-C15-C22	**-61.3**	**-108.8**	**-98.1**	**-101.9**	**-112.4**	**-98.0**	**-101.8**	**-112.4**	**-98.1**	**-101.8**	**-112.3**	**-98.7**
O29-C22	**1.2**	**1.2**	**1.2**	**1.2**	**1.2**	**1.2**	**1.2**	**1.2**	**1.2**	**1.2**	**1.2**	**1.2**
O29-C22-O30	**122.2**	**124.4**	**122.6**	**124.0**	**123.2**	**122.8**	**124.0**	**123.2**	**122.8**	**124.0**	**123.2**	**122.8**
O29-C22-O30-C35	**3.9**	**2.4**	**1.8**	**0.3**	**0.6**	**0.2**	**0.3**	**0.7**	**0.3**	**0.3**	**0.7**	**0.3**
N21-C27	**1.5**	**1.5**	**1.5**	**1.5**	**1.5**	**1.5**	**1.5**	**1.5**	**1.5**	**1.5**	**1.5**	**1.5**
N21-C27-C34	**111.5**	**110.4**	**111.6**	**114.4**	**113.3**	**111.4**	**114.4**	**113.3**	**111.4**	**114.4**	**113.4**	**111.5**
N21-C27-C34-O43	**-178.2**	**-177.4**	**-171.7**	**-159.8**	**-162.5**	**-173.6**	**-159.8**	**162.5**	**-173.6**	**-159.8**	**-162.2**	**-173.2**
O43-C34	**1.5**	**1.5**	**1.5**	**1.5**	**1.5**	**1.5**	**1.5**	**1.5**	**1.5**	**1.5**	**1.5**	**1.5**
O43-C34-C44	**111.4**	**109.1**	**109.1**	**111.0**	**109.4**	**108.7**	**111.0**	**109.4**	**108.7**	**111.0**	**109.4**	**108.7**
O43-C34-C44-C54	**59.3**	**53.8**	**58.8**	**65.6**	**61.9**	**58.2**	**65.6**	**62.0**	**58.1**	**65.6**	**62.0**	**58.0**
O47-C37	**1.4**	**1.4**	**1.4**	**1.4**	**1.4**	**1.4**	**1.4**	**1.4**	**1.4**	**1.4**	**1.4**	**1.4**
O47-C37-C45	**123.2**	**120.4**	**120.4**	**118.7**	**120.1**	**120.7**	**118.7**	**120.1**	**120.7**	**118.7**	**120.1**	**120.7**
O47-C37-C45-N56	**3.8**	**-1.6**	**-2.4**	**5.1**	**-2.9**	**-2.3**	**5.1**	**-2.9**	**-2.3**	**5.1**	**-2.8**	**-2.3**

4th method shows that this angle increases in both solvent and gas phases but the increasing angle in gas phase is stranger than solvent. Fifth and sixth methods show the same changes of angle in gas and solvent phases. The results of full geometry optimization with the Onsager model of the molecule are presented (Table 1). The comparison between vacuum and 3 solvents with different dielectric constants at three basis sets has shown only a relatively small change of the geometrical parameters for vinblastine structure.

Table 2. Calculated functions of harmonic frequencies (cm^{-1}), IR intensities (km/mol), Dipole Moments (μ, Debye) and ΔE, ΔH, ΔG in kcal/mol and ΔS in cal/mol.K^{-1}.

T(k)	1/ε	Normal mode	B3LYP						HF					
			6-31g**			6-31g*			6-31g**			6-31g*		
			μ	Ln[I]	Ln[F]	μ	Ln[I]	Ln[F]	μ	Ln[I]	Ln[F]	μ	Ln[I]	Ln[F]
300, 305, 310, 315, 320	1/78.39	6		-5.09	1.06		-5.13	0.74		6.18	4.62		6.18	4.62
		7	1.7691	5.74	3.81	1.7768	5.74	3.82	1.8969	0.66	5.16	1.9035	0.81	5.18
		14		5.36	6.40		5.36	6.40		5.51	6.48		5.48	6.48
	1/32.63	6		-5.4	0.08		-9.21	-1.33		6.18	4.6		6.18	4.61
		7	1.7682	5.74	3.78	1.7759	5.74	3.8	1.8965	0.66	5.15	1.9032	0.81	5.18
		14		5.35	6.39		5.36	6.39		5.49	6.47		5.46	6.48
	1/24.55	6		-5.36	-0.22		-5.38	-9.21		6.18	4.62		6.18	4.62
		7	1.7719	5.74	3.81	1.7796	5.73	3.82	1.8999	0.68	5.15	1.9066	0.83	5.17
		14		5.36	6.40		5.37	6.40		5.51	6.47		5.49	6.48
			B3LYP						HF					
			6-31g**			6-31g*			6-31g**			6-31g*		
300	1/78.39	ΔE	-810.71			-807.14			-5.42			-1.02		
		ΔH	-810.11			-806.55			-4.82			-0.42		
		ΔG	-830.52			-827.01			-24.46			-20.03		
		ΔS	68.01			68.22			65.44			65.36		
	1/32.63	ΔE	-810.63			-807.06			-5.29			-0.89		
		ΔH	-810.03			-806.46			-4.7			-0.29		
		ΔG	-830.5			-827.02			-24.33			-19.91		
		ΔS	68.23			68.51			65.46			65.38		
	1/24.55	ΔE	-810.68			-807.11			-5.41			-1.02		
		ΔH	-810.08			-806.51			-4.82			-0.42		
		ΔG	-830.65			-827.2			-24.47			-20.04		
		ΔS	68.54			68.96			65.49			65.40		
305	1/78.39	ΔE	-810.64			-807.07			-5.36			-0.95		
		ΔH	-810.03			-806.47			-4.75			-0.35		
		ΔG	-830.86			-827.35			-24.79			-20.36		
		ΔS	68.27			68.48			65.68			65.60		
	1/32.63	ΔE	-810.56			-806.99			-5.23			-0.83		
		ΔH	-809.95			-806.38			-4.62			-0.22		
		ΔG	-830.84			-827.36			-24.66			-20.24		
		ΔS	68.50			68.77			65.70			65.62		
	1/24.55	ΔE	-810.61			-807.04			-5.35			-0.95		
		ΔH	-810			-806.43			-4.74			-0.35		
		ΔG	-830.99			-827.55			-24.79			-20.37		
		ΔS	68.81			69.22			65.73			65.64		
310	1/78.39	ΔE	-810.57			-807			-5.29			-0.89		
		ΔH	-809.95			-806.39			-4.68			-0.28		
		ΔG	-831.2			-827.7			-25.11			-20.69		
		ΔS	68.53			68.74			65.92			65.84		
	1/32.63	ΔE	-810.49			-806.92			-5.16			-0.76		
		ΔH	-809.87			-806.3			-4.55			-0.15		
		ΔG	-831.18			-827.7			-24.99			-20.56		
		ΔS	68.76			69.03			65.94			65.86		
	1/24.55	ΔE	-810.54			-806.97			-5.29			-0.89		
		ΔH	-809.92			-806.35			-4.67			-0.27		
		ΔG	-831.33			-827.89			-25.12			-20.7		
		ΔS	69.07			69.48			65.97			65.88		
315	1/78.39	ΔE	-810.5			-806.93			-5.23			-0.83		
		ΔH	-809.87			-806.31			-4.6			-0.2		
		ΔG	-831.54			-828.04			-25.44			-21.02		
		ΔS	68.79			69			66.16			66.08		
	1/32.63	ΔE	-810.42			-806.85			-5.1			-0.7		
		ΔH	-809.79			-806.22			-4.47			-0.07		
		ΔG	-831.53			-828.05			-25.32			-20.89		
		ΔS	69.01			69.29			66.18			66.10		
	1/24.55	ΔE	-810.47			-806.9			-5.22			-0.82		
		ΔH	-809.84			-806.27			-4.6			-0.2		
		ΔG	-831.68			-828.24			-25.45			-21.3		
		ΔS	69.33			69.74			66.21			66.12		
320	1/78.39	ΔE	-810.43			-806.86			-5.16			-0.77		
		ΔH	-809.79			-806.22			-4.53			-0.13		
		ΔG	-831.89			-828.39			-25.78			-21.35		
		ΔS	69.05			69.26			66.4			66.31		
	1/32.63	ΔE	-810.34			-806.78			-5.03			-0.64		

	ΔH	-809.71	-806.14	-4.4	-0.00
	ΔG	-831.88	-828.4	-25.65	-21.22
	ΔS	69.27	69.55	66.42	66.33
1/24.55	ΔE	-810.4	-806.83	-5.16	-0.76
	ΔH	-809.76	-806.19	-4.52	-0.12
	ΔG	-832.03	-828.59	-25.78	-21.36
	ΔS	69.58	70	66.45	66.36

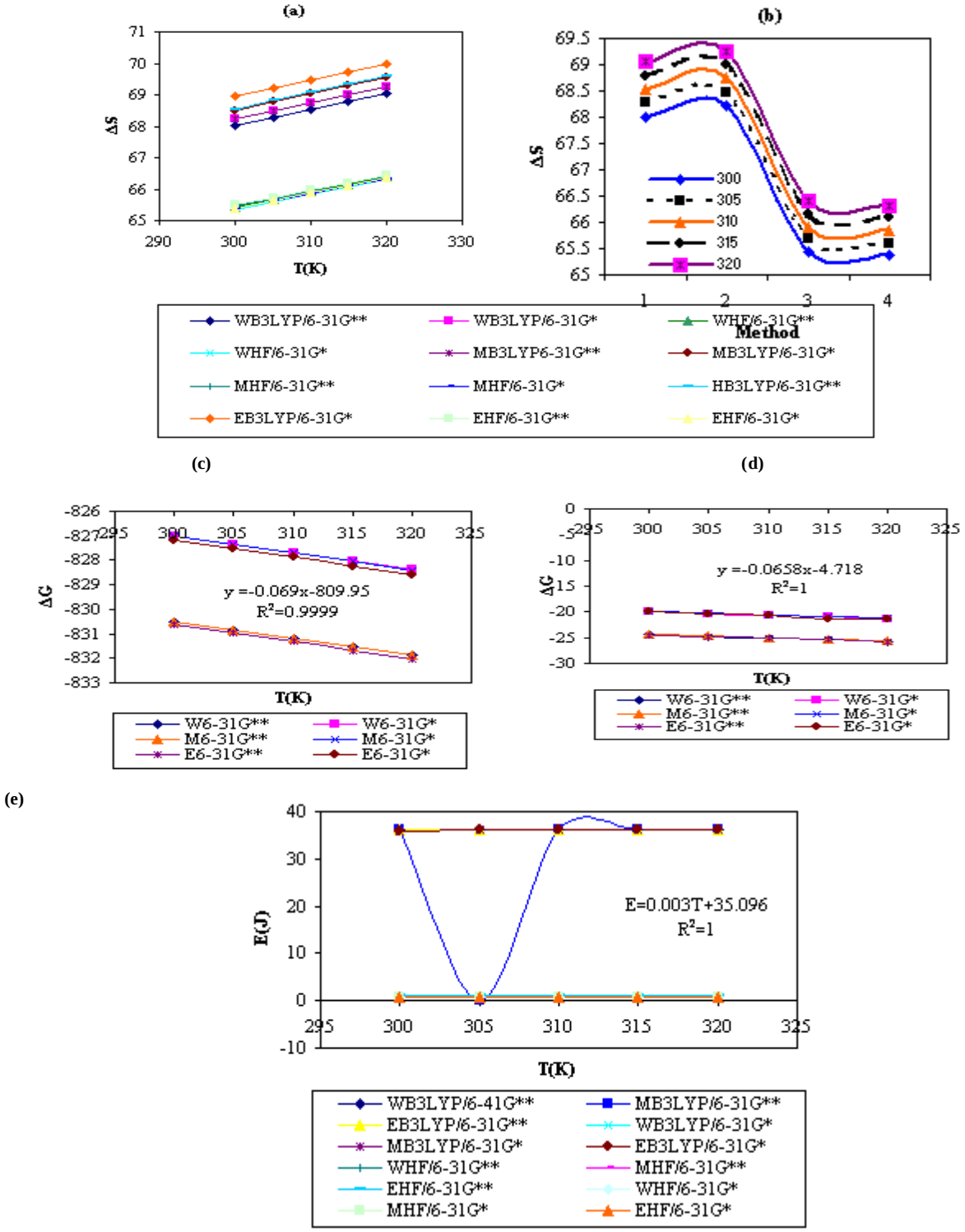

Fig.3. Calculated ΔS in different media via **(a)** temperature **(b)** methods , optimized Gibbs free energy **(c)** B3LYP **(d)** HF levels of theory which performed by various basis sets (6-31G*,6-31G**) , dielectric and **(e)** changes of electro motive force via temperature (Water, Ethanol and Methanol).

The DFT calculated geometric parameters and relative total energies in (kcal/mol) at HF and B3LYP levels of the optimized structure, for vinblastine are compared in Table 1. The bond length calculated for N12-C13 at the HF level range from 1.4 to 1.5 Å, at the B3LYP level is 1.4 Å. The bond length calculated for O29-C22 at the HF and B3LYP levels is 1.2 Å. The bond length calculated for N21-C27 at the HF level range from 1.4 to 1.5Å, at the B3LYP level is 1.5 Å. The bond length calculated for O43-C34 at the HF level range from 1.4 to 1.5 Å, at the B3LYP level is 1.5 Å. The bond length calculated for O47-C37 at the HF and B3LYP levels is 1.4 Å. The calculations of the relative Harmonic frequencies, IR intensities, dipole moments and ΔH, ΔG, ΔS for active points of vinblastine are presented in Table 2. The frequency ratios (cm^{-1}), intensity (km/mol), dipole moments (Debye), ΔH, ΔG kcal/mol and ΔS ($cal/mol.K^{-1}$) indicate the consistency between the two calculation methods (DFT/HF). The highest and lowest values of variations of entropy indicated by different methods in fig. 3 a via T(K) and b via method can be observed in various basis sets and dielectric constants. The entropy variations increase with temperature in water, ethanol and methanol (fig. 3 a). The largest values of entropy variation is related B3LYP/6-31G* and the smallest values can be seen in HF/6-31G* method. The value of ΔS increases with temperature. As for fig. 3b which demonstrates entropy variations several solvents, results obtained by 3th method is in conformity with 4th method. Linear relations can be observed between temperature and ΔS, which these parameters increase with temperature. The pathway of energy and potential variations are close to each other in different solvents and the largest values can be seen in water. As for ΔS, ethanol has largest values in magnitude rather than other solvents. As is shown in fig. 3 c,d , the variation of Gibbs Free energy behave in the same way in water, methanol and ethanol solvents at B3LYP and HF levels, respectively. As it is obvious in fig. 3 c, d, these parameters which are obtained by relation coefficient R^2=0.9999 (fig. 3 c) for B3LYP and R^2=1 (fig. 3 d) for HF . In fig.3, we have observed that by increasing temperature ΔG is decreased in two levels. Also, the value of electromotive force, E (v), decreases with temperature in different solvents (fig.3e). These values in ethanol which behaves somewhat differently than water and methanol are lower rather than other solvents.
According to table 2, dipole moment, intensity and frequency of the structure of vinblastine don't change in several temperature (300,305,310,315 and 320K), but noticeable variations can be observed in these parameters in different methods.The correlation of thermodynamic parameters is biochemical significant, rather than due to statistical artifact.

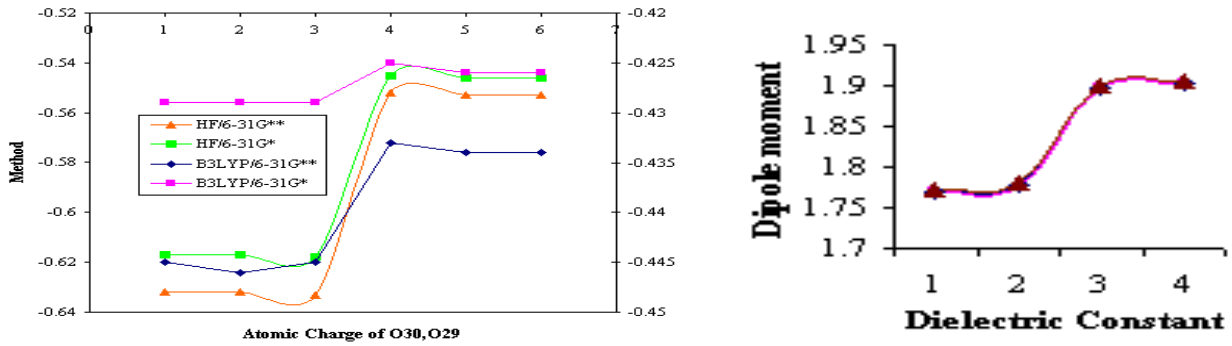

Fig.4. Total atomic charge of O30 (1,2,3 on x axis) , O29 (4,5,6 on x axis) (active centers) and dipole moment of vinblastine at different levels of theory.

In the study presented here, the high level of Gibbs free energy and electromotive force correlation and significance (R2) for all these compounds indicates that similar processes are involved regardless of the nature of their chemical environment. Note that the slope of the ΔH–ΔS or the compensation temperature is different from the mean temperature over which the parameters were estimated.

Table 3. Total atomic charges of the structures.

T(k)	1/ε	Atom	Total atomic charges			
			B3LYP		HF	
			6-31g**	6-31g*	6-31g**	6-31g*
300	1/78.39	C22	0.436	0.382	0.617	0.556
		O29	-0.433	-0.425	-0.552	-0.545
		O30	-0.445	-0.429	-0.632	-0.617
		C35	-0.084	-0.216	-0.022	-0.175
		H50	0.13	0.173	0.141	0.191
		H51	0.138	0.178	0.144	0.191
		H52	0.139	0.179	0.145	0.193
	1/32.63	C22	0.436	0.382	0.617	0.556
		O29	-0.434	-0.426	-0.553	-0.546
		O30	-0.446	-0.429	-0.633	-0.617
		C35	-0.084	-0.216	-0.022	-0.175
		H50	0.13	0.173	0.142	0.191
		H51	0.138	0.178	0.144	0.191
		H52	0.139	0.179	0.145	0.193
	1/24.55	C22	0.436	0.382	0.617	0.556
		O29	-0.434	-0.426	-0.553	-0.546
		O30	-0.446	-0.429	-0.633	-0.616
		C35	-0.084	-0.216	-0.022	-0.175
		H50	0.13	0.173	0.142	0.191
		H51	0.138	0.178	0.144	0.191
		H52	0.139	0.179	0.145	0.193
305	1/78.39	C22	0.436	0.382	0.617	0.556
		O29	-0.433	-0.425	-0.552	-0.545
		O30	-0.445	-0.429	-0.632	-0.617
		C35	-0.084	-0.216	-0.022	-0.175
		H50	0.13	0.173	0.141	0.191
		H51	0.138	0.178	0.144	0.191
		H52	0.139	0.179	0.145	0.193
	1/32.63	C22	0.436	0.382	0.617	0.556
		O29	-0.434	-0.426	-0.553	-0.546
		O30	-0.446	-0.429	-0.633	-0.617
		C35	-0.084	-0.216	-0.022	-0.175
		H50	0.13	0.173	0.141	0.191
		H51	0.138	0.178	0.144	0.191
		H52	0.139	0.179	0.145	0.193
	1/24.55	C22	0.436	0.382	0.617	0.556
		O29	-0.434	-0.426	-0.553	-0.546
		O30	-0.446	-0.429	-0.633	-0.618
		C35	-0.084	-0.216	-0.022	-0.175
		H50	0.13	0.173	0.142	0.191
		H51	0.138	0.178	0.144	0.191
		H52	0.139	0.179	0.145	0.193
310	1/78.39	C22	0.436	0.382	0.617	0.556
		O29	-0.433	-0.425	-0.552	-0.545
		O30	-0.445	-0.429	-0.632	-0.617
		C35	-0.084	-0.216	-0.022	-0.175
		H50	0.13	0.173	0.141	0.191
		H51	0.137	0.178	0.144	0.191
		H52	0.139	0.179	0.145	0.193
	1/32.63	C22	0.436	0.382	0.617	0.556
		O29	-0.434	-0.426	-0.553	-0.546
		O30	-0.446	-0.429	-0.632	-0.617
		C35	-0.084	-0.216	-0.022	-0.175
		H50	0.13	0.173	0.141	0.191
		H51	0.138	0.178	0.144	0.191
		H52	0.139	0.179	0.145	0.193
	1/24.55	C22	0.436	0.382	0.617	0.556
		O29	-0.434	-0.426	-0.553	-0.546
		O30	-0.445	-0.429	-0.633	-0.618
		C35	-0.084	-0.216	-0.022	-0.175
		H50	0.13	0.173	0.142	0.191
		H51	0.138	0.178	0.144	0.191
		H52	0.139	0.179	0.145	0.193

T(k)	1/ε	Atom	Total atomic charges			
			B3LYP		HF	
			6-31g**	6-31g*	6-31g**	6-31g*
315	1/78.39	C22	0.436	0.382	0.617	0.556
		O29	-0.433	-0.425	-0.552	-0.545
		O30	-0.445	-0.4295	-0.632	-0.617
		C35	-0.084	-0.216	-0.022	-0.175
		H50	0.13	0.173	0.141	0.191
		H51	0.138	0.178	0.144	0.191
		H52	0.139	0.179	0.145	0.193
	1/32.63	C22	0.436	0.382	0.617	0.556
		O29	-0.434	-0.426	-0.553	-0.546
		O30	-0.446	-0.429	-0.63	-0.617
		C35	-0.084	-0.216	-0.022	-0.175
		H50	0.13	0.173	0.141	0.191
		H51	0.138	0.178	0.144	0.191
		H52	0.139	0.179	0.145	0.193
	1/24.55	C22	0.436	0.382	0.617	0.556
		O29	-0.434	-0.426	-0.553	-0.546
		O30	-0.446	-0.429	-0.633	-0.618
		C35	-0.084	-0.216	-0.022	-0.175
		H50	0.13	0.173	0.142	0.191
		H51	0.138	0.178	0.144	0.191
		H52	0.139	0.179	0.145	0.193
320	1/78.39	C22	0.436	0.382	0.617	0.556
		O29	-0.433	-0.425	-0.552	-0.545
		O30	-0.445	-0.429	-0.632	-0.617
		C35	-0.084	-0.216	-0.022	-0.175
		H50	0.13	0.173	0.141	0.191
		H51	0.138	0.178	0.144	0.191
		H52	0.139	0.179	0.145	0.193
	1/32.63	C22	0.436	0.382	0.617	0.556
		O29	-0.434	-0.426	-0.553	-0.546
		O30	-0.446	-0.429	-0.633	-0.617
		C35	-0.084	-0.216	-0.022	-0.175
		H50	0.13	0.173	0.141	0.191
		H51	0.138	0.178	0.144	0.191
		H52	0.139	0.179	0.145	0.193
	1/24.55	C22	0.436	0.382	0.617	0.556
		O29	-0.434	-0.426	-0.553	-0.546
		O30	-0.446	-0.429	-0.633	-0.618
		C35	-0.084	-0.216	-0.022	-0.175
		H50	0.13	0.173	0.142	0.191
		H51	0.138	0.178	0.144	0.191
		H52	0.139	0.179	0.145	0.193

O29 and O30 are the only atoms of active site of vinblastine which are sensitive to solvent and temperature, and their atom charge change with these parameters (Fig.4). But as it can be observed in table 3 there are no remarkable

variations in other atom with changing these parameters. Fig.4 demonstrates the effects of methods and basis set on O29 and O30 atom charge. The values concluded by B3LYP are larger than HF method. Fig.5 a, b, c demonstrates the relationship between intensity (a, b, c), frequency (d) and normal mode. This figure shows that the variation of intensity with normal mode in HF and B3LYP methods are different from each other in B3LYP method .The value of intensity in normal mode of 7 has larger value than another method, and vice versa, the normal mode of 6 has smaller value in B3LYP method. But as it is obvious in fig.5 a, b, c, intensity in normal mode of 14 shows the same situation and maximum value in both of these methods.

In B3LYP method the variation of intensity with normal mode in different solvents are close to each other. Also, the results obtained by HF method are similar to B3LYP.

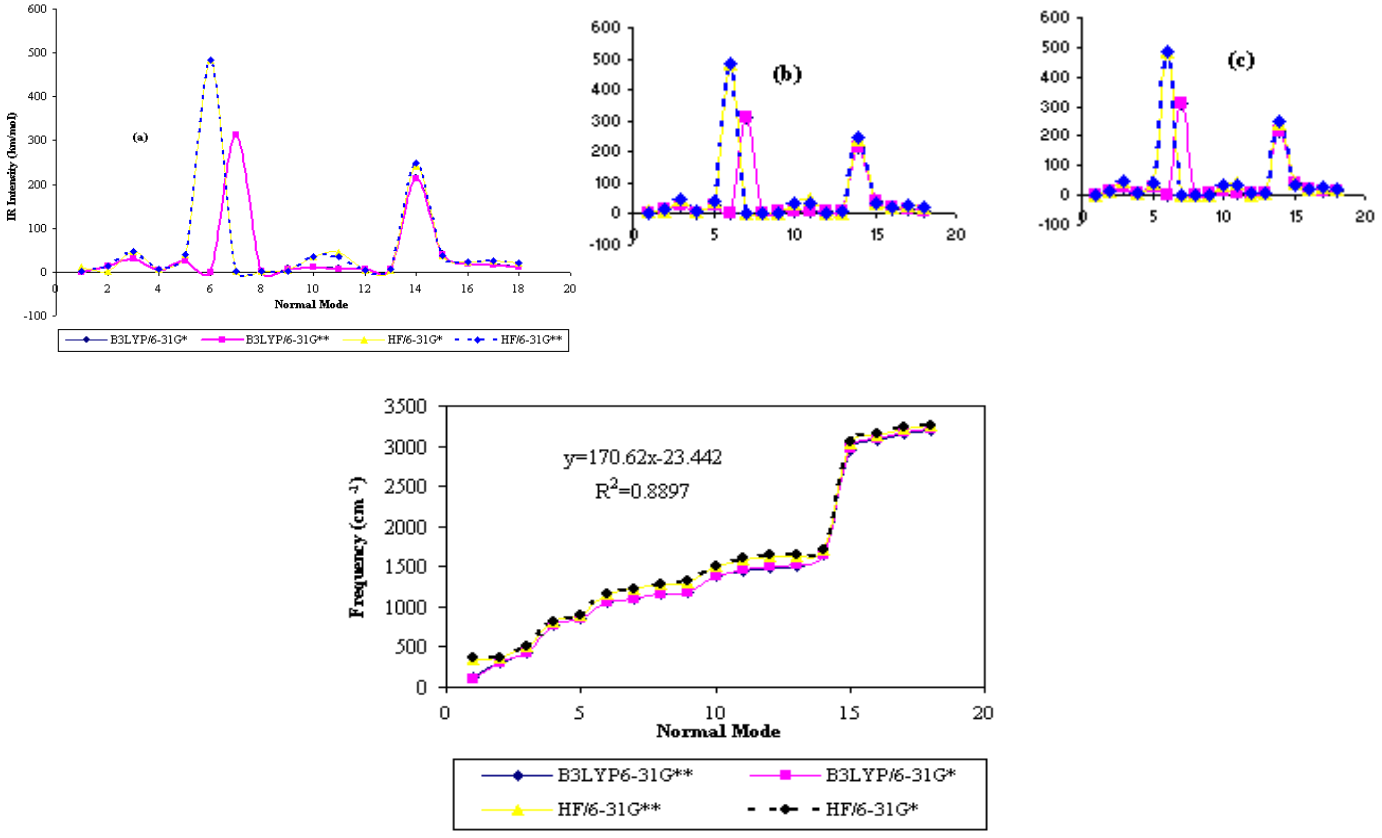

(d)

Fig.5. Changes of IR intensity versus normal modes in **(a)** water **(b)** Methanol and **(c)** Ethanol media at various levels of theory, **(d)** Frequencies vs. normal mode which performed by B3LYP/6-31G** in different solvents at 310 K.

A remarkable changing can be observed with going from 14 to 15 normal modes in all of the methods, solvents and temperatures. The variation of frequency as a function of normal mode are plotted in fig.5 d Similar to intensity. Changing methods led to variation of frequency, but the effect of changing solvents are not noticeable.

Conclusion

This investigation predicted that full geometry optimization of vinblastine and the vibrational frequencies for the main part of structure could be successfully elucidated by the HF and B3LYP theoretical levels using basis sets.

On the basis of the results of these studies we conclude the following:

- By optimization of this molecule in gas and solvent phases remarkable variations in bond angle and torsion angle can be seen, but no change was observed in bond distances.
- Among the active part of molecule, only the atom charge of O29and O30 change.
- The most intensity of normal mode of 7 and 14, was obtained by B3LYP method and about normal mode of 6 and 14, the largest value can be seen in HF method. But no effect was seen in these normal modes with variations of temperature.
- A remarkable changing can be observed with going from 14 to 15 normal mode in all of the methods and temperatures.
- ΔS, ΔH and E (v) values increase with temperatures but ΔG decreases. But the variations of solvent and temperature have a considerable effect on ΔS.
- It is shown that dipole moment for the structure obtained by B3LYP has minimum value and maximum value can be find by HF method.

Therefore, this study confirms that the theoretical calculation of the vibrational frequencies and thermodynamic properties for vinblastine is quite useful for predicting stability of indicated structure in various media. In this work, we have quantitative comparison of vinblastine with the new environment by theoretical methods. These data allow us to cautiously correlate the clinical effects of this compound with their overall affinity for the site of action.

References

[1] Sh. Lobert, J. W. Ingram and J. J. Correia, The thermodynamics of vinca alkaloid-induced tubulin spirals formation, Biophysical chemistry, 2006, 126, 50-58.

[2] Sh. Lobert, J. W. Ingram and J. J. Correia, Additivity of Dilantin and Vinblastine Inhibitory Effects on Microtubule Assembly1, cancer research, 1999, 59, 4816-4822.

[3] J. C. Lee, D. Harrison and S. N. Timasheff, Interaction of vinblastine with calf brain microtubule protein, Biological Chemistry, 1975, Vol. 250, No. 24, pp. 9276-9282.

[4] J. J. Correia and S. Lobert, Physiochemical aspects of tubulin- interacting antimitotic drugs, Current pharmaceutical design, 2001, 7, 1213-1228.

[5] Sh. Lobert, B. Vulevic and J. J. Coreia, Interaction of vinca alkaloids with tubulin: a comparison of vinblastine, vincristine and vinorelbine, Biochemistry, 1996, 35, 6806-6814.

[6] S. S. Rai and J. Wolff, Localization of the vinblastine- binding site on β- tubulin, Biological chemistry, 1996, Vol. 271, No. 25, 14707-14711.

[7] Z. D. Szafran, A. Katrusiak and M. Szafran, Molecular structure of quinuclidine betaine hydrate studied by X- ray diffraction, DFT, FTIR, Raman, NMR methods, Molecular structure, 2009, 921, 295-299.

[8] A. E. Ozel, S. Celik and S. Akyuz, Vibrational spectroscopic investigation of free and coordinated 5-aminoquinoline: The IR, raman and DFT studies, Molecular structure, 2009, 523- 530.

[9] K. Balci, A. Koch and E. Kleinpeter, A theoretical IR spectroscopic study based on DFT calculations for free mn-$15S_2O_3$ maleonitrile- dithiacrown ether compound, Molecular structure, 2009, 919, 128-139.

[10] A. Tarajko, H. Cybulski, M. J. Chmielewski, J. Bukowska and M. Skompska, Electrochemical and spectroscopic characterization of poly (1, 8-diaminocarbazole): Part I. Electropolymerization and determination of the polymer structure by FTIR studies and DFT calculations, Electrochimica acta, 2009.Sh. Lobert, J. W. Ingram and J. J. Correia, Additivity of Dilantin and Vinblastine Inhibitory Effects on Microtubule Assembly1, cancer research, 1999, 59, 4816-4822.

[11] V. S. Madhavan, H. T. Varghese, S. Mathew, J. Vinsova and C. Y. Panicker, FT-IR, FT-Raman and DFT calculations of 4-chloro-2-(3,4-dichlorophenylcarbamoyl)phenyl acetate, Spectrochimica acta, 2009, 72, 547-553.
[12] V. L. Furer, I. I. Vandyukova, A. E. Vandyukova, J. P. Majoral, A. M. Caminade and V. I. Kovalenko, DFT study of structure, IR and Raman spectra of P00 and P04 dendrimers built from octasubstituted metal-free phthalocyanine core Chemical physics, 2009, 358, 177-183.
[13] T. Dziembowska, M. Szafran, A. Katrusiak and Z. Rozwadowski, Crystal structure of and solvent effect on tautomeric equilibrium in Schiff base derived from 2-hydroxy-1-naphthaldehyde and methylamine studied by X-ray diffraction, DFT, NMR and IR methods, Molecular structure, 2009.
[14] M. Snehalatha, C. Ravikumar, I. H. Joe, N. Sekar and V. S. Jayakumar, Spectroscopic analysis and DFT calculations of a food additive Carmoisine, Spectrochimica acta, 2009, 72, 654-662.
[15] M.J. Frisch, G.W. Trucks, H.B. Schlegel, G.E. Scuseria, M.A. Robb, J.R. Cheeseman, J.A. Montgomery Jr., T. Vreven,K.N. Kudin, J.C. Burant, J.M. Millam, S.S. Iyengar, J. Tomasi, V. Barone, B.
Mennucci, M. Cossi, G. Scalmani, N. Rega, G.A. Petersson, H. Nakatsuji, M. Hada, M. Ehara, K. Toyota, R. Fukuda, J. Hasegawa, M. Ishida, T.Nakajima, Y. Honda, O. Kitao, H. Nakai, M. Klene, X. Li, J.E. Knox, H.P.Hratchian, J.B. Cross, V. Bakken, C.Adamo, J. Jaramillo, R. Gomperts, R.E. Stratmann, O. Yazyev, A.J. Austin, R. , C. Pomelli, J.W. Ochterski, P.Y. Ayala, K.Morokuma, G.A. Voth, P. Salvador, J.J. Dannenberg, V.G. Zakrzewski, S. Dapprich, A.D. Daniels, M.C. Strain, O. Farkas, D.K. Malick, A.D. Rabuck, K. Raghavachari, J.B. Foresman, J.V. Ortiz, Q. Cui, A.G. Baboul, S. Clifford, J. Cioslowski, B.B. Stefanov, G. Liu, A. Liashenko, P. Piskorz, I. Komaromi, R.L . Martin, D.J. Fox, T. Keith, M.A. Al- Laham, C.Y. Peng, A. Nanayakkara, M. Challacombe, P.M.W. Gill, B. Johnson,W. Chen, M.W. Wong, C. Gonzalez, J.A. Pople, GAUSSIAN 03, Revision D.02, Gaussian, Inc., Wallingford, CT, 2004.
[16] A.D. Becke, J. Chem. Phys. 98 (1993) 5648.
[17] A.D. Becke, J. Chem. Phys. 107 (1997) 8554.
[18] C. Lee, W. Yang, G.R. Parr, Phys. Rev. B 37 (1988) 785.
[19] W.J. Hehre, L. Random, P.V.R. Schleyer, J.A.Pople, Ab Initio Molecular Orbital Theory, Wiley, New York, 1986.
[20] G. Cohen and H. Eisenberg, Biopolymers 6 (1968) 1077.
[21] P. Beak, J. B. Covington, S. G. Smith, J. M. White and J. M. Zeiger, J. Org. Chem. 45 (1980) 1354.
[22] E. Westhof and D.L. Beveridge, In Water Science Reviews, F. Francs (ed), Cambridge University Press, New York, 1989, vol. 1.
[23]X. C. Wang, J. Nichols, M. Feyereisen, M. Gutovski, J. Boatz, A. D. J. Haymet and J. Simons, J. Phys. Chem. 95 (1991) 10419.
[24] J. S. Craw, J. M. Guest, M. D. Cooper, N. A. Burton and I. H. Hillier, J. Phys. Chem. 100 (1996) 6304.
[25] S. Scheiner and L. Wang, J. Am. Chem. Soc. 115 (1993) 1958.
[26] S. Scheiner and X. Duang, Biophys. J. 60 (1991) 874.
[27] Kirkwood, J. G. J. Chem. Phys. 1934, 2, 767.
[28] Kirkwood, J. G. J. Chem. Phys. 1939, 7, 911.
[29]Onsager, L. J. Am. Chem. Soc. 1936, 58, 1486.
[30] Wong, M. A.; Frisch, M. J.; Wiberg, K. B. J. Am. Chem. Soc. 1991, 113, 4776.
[31] Wong, M. A.; Frisch, M. J.; Wiberg, K. B. J. Am. Chem. Soc. 1992, 114, 523.